

PROJECT OF THE COMPACT SUPERCONDUCTING STORAGE RING SIBERIA-SM

V.V. ANASHIN, V.S. ARBUZOV, G.A. BLINOV, V.G. VESHCHEREVICH, P.D. VOPLY,
E.I. GORNIKER, N.I. ZINEVICH, E.I. ZININ, N.I. ZUBKOV, V.A. KISELEV, E.P. KOLLEROV,
G.N. KULIPANOV, Yu.G. MATVEEV, A.S. MEDVEDKO, N.A. MEZENTSEV, L.G. MORGUNOV,
V.M. PETROV, S.P. PETROV, V.V. REPKOV, V.A. ROENKO, A.N. SKRINSKY, S.V. SUKHANOV,
Yu.I. TOKAREV and E.M. TRAKHTENBERG

Institute of Nuclear Physics, 630090 Novosibirsk, USSR

In the last decade researches dealing with the creation of technology for X-ray lithography and for appropriate production equipment have been performed in many countries. The basic aim of these works is to provide a mass production of inexpensive devices with submicron structures ($0.7\text{--}0.1\ \mu\text{m}$). Bringing X-ray lithographic technology into commercial practice necessitates to design and build a dedicated SR source for the electronic industry. The use of superconducting bending magnets with $40\text{--}70\ \text{kG}$ field strength enables the storage ring circumference to be reduced by a factor of $2\text{--}5$ and the injection energy by a factor of $3\text{--}4$ as compared to the conventional designs of storage rings. In the present paper we consider a storage ring which was designed for a maximum energy of $600\ \text{MeV}$, with $60\ \text{kG}$ field strength in its bending magnets and $10\ \text{m}$ circumference. The critical SR wavelength is $8.6\ \text{\AA}$. The electrons are injected into the storage ring at $50\text{--}60\ \text{MeV}$ and the maximum stored current is assumed to be equal to $0.3\ \text{A}$.

1. Magnetic system of the storage ring

The magnetic system of the storage ring comprises four superperiods, each containing two superconducting 45° bending magnets and three quadrupole lenses placed mirror-symmetrically (fig. 1). At the edges of the superperiods there are straight sections intended for some elements of the injection and beam control systems, an rf cavity and sextupole lenses [1].

The bending magnets are of the rectangular type with parallel edges. At a maximum energy of $600\ \text{MeV}$ the magnetic field is equal to $60\ \text{kG}$. These magnets create an additional edge focusing of the electron beam in the vertical direction. To obtain as low emittance as possible, all quadrupole lenses in this structure are focusing in the radial direction. Fig. 2 shows the betatron functions $\beta_x(s)$ and $\beta_z(s)$ and the dispersion function $\eta_x(s)$ throughout the superperiod.

The working betatron frequencies ν_x and ν_z are taken equal to 2.6 and 1.12 , respectively. In this case, the horizontal emittance is minimal (at $600\ \text{MeV}$ energy, $\epsilon_x = 8.5 \times 10^{-6}\ \text{cm rad}$) and the conditions for a one-turn injection in the vertical direction are optimal.

The straight sections I, III and II, IV (fig. 1) are 60 and $40\ \text{cm}$ long, respectively. The difference in their length permits the storage ring chromaticity to be completely compensated for: $\xi_x = -1.54$ and $\xi_z = 0.225$ at the injection energy. This is done with the aid of the

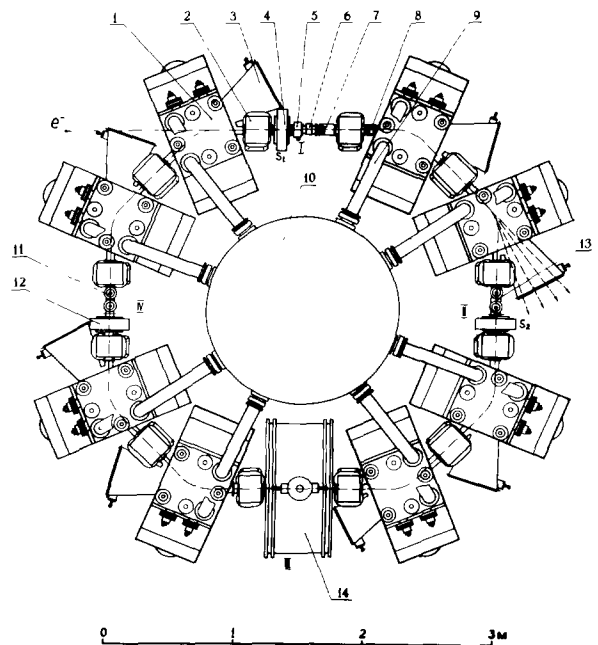


Fig. 1. Layout of the storage ring: (1) superconducting magnet, (2) quadrupole lens, (3) SR extraction chamber, (4) sextupole lens, (5) beam current pickup, (6) meter of betatron oscillation frequencies, (7) 40° input magnet, (8) 4° input magnet, (9) helium pipe line, (10) helium-supplying reservoir, (11) pre-injector, (12) octupole lens, (13) inflector, (14) rf cavity.

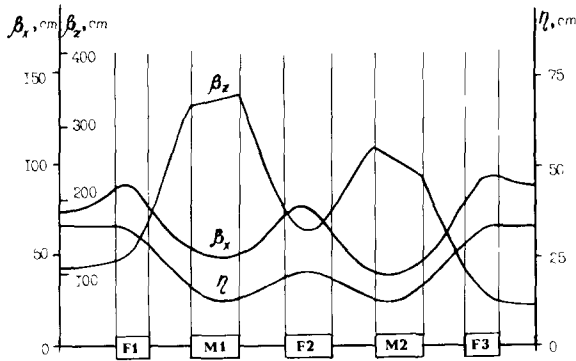


Fig. 2. Betatron functions β_x , β_z and dispersion function η for one superperiod.

s sextupole lenses S_1 and S_2 positioned in the straight sections I and II, where the values of the β -functions are not equal with respect to x and z :

$$\beta_{xI} \neq \beta_{xII}, \quad \beta_{zI} \neq \beta_{zII}.$$

The storage ring orbit is corrected by additional windings on the magnetic elements: on the poles of the quadrupole lenses for vertical correction and in the bending magnets for horizontal correction.

The aperture of the vacuum chamber is taken to be equal to ± 20 mm and ± 12 mm, respectively, in the horizontal and vertical directions. These parameters have been chosen after taking into account the betatron oscillations of electrons, energy variation, requirements for the injection aperture, as well as the tolerances on the distortions of the closed orbit. The basic parameters of the storage ring are listed in table 1.

A version of the superconducting magnet has been developed which comprises three superconducting windings (1–3), a central cold pole (4, 5) and a warm yoke intended to close the magnetic flux (fig. 3). Winding 1 is the basic winding, and it is switched on after the saturation of the ferromagnetic material of the central pole. In addition, it should generate the field from 20 to 60 kG. Winding 2 serves to compensate for the influence of the interpole gap on the field inhomogeneity in the magnet and to generate a 0–20 kG magnetic field. Winding 3 is necessary to compensate for the influence of the side gaps between the cold and warm sections of the magnetic circuit. The parameters of the magnet are listed in table 2.

Synchrotron radiation is completely extracted from the low-temperature region of the cryostat of the magnet not reaching the nitrogen screen (fig. 4). All of the cryostat surfaces, which face the vacuum, are stainless steel and the cryostat walls, contiguous with the warm yoke, are bimetallic (Armco/stainless steel), and the nitrogen screens are made of copper [2].

The helium volume is assembled with a nitrogen bath and nitrogen screens and suspended from the

Table 1
Basic parameters of the storage ring

Energy E [MeV]	600
Circumference [m]	10
Number of superperiods	4
Number of dipoles	8
Guiding magnetic field B [kG]	60
Bending radius ρ [cm]	33
Number of quadrupoles	12
Number of sextupoles	2
Betatron numbers ν_x, ν_z	2.6, 1.12
Momentum compaction factor α	0.0822
Chromaticity ξ_x, ξ_z	-1.54, 0.225
Horizontal emittance ϵ_x [cm rad]	8.5×10^{-6}
Damping times τ_z, τ_x, τ_y [ms]	1.25, 1.25, 0.625
RMS energy spread σ_E/E	8.7×10^{-4}
Energy losses per turn, ΔW [keV]	31.6
Revolution frequency f_0 [MHz]	30
Harmonic number q	1
Rf voltage amplitude U_{rf} [kV]	100
Beam current I [mA]	300
Lifetime at 300 mA beam current, τ [h]	4.4
Bunch length σ_t [cm]	8
Critical SR wavelength λ_c [Å]	8.6
Injection energy E_{inj} [MeV]	60

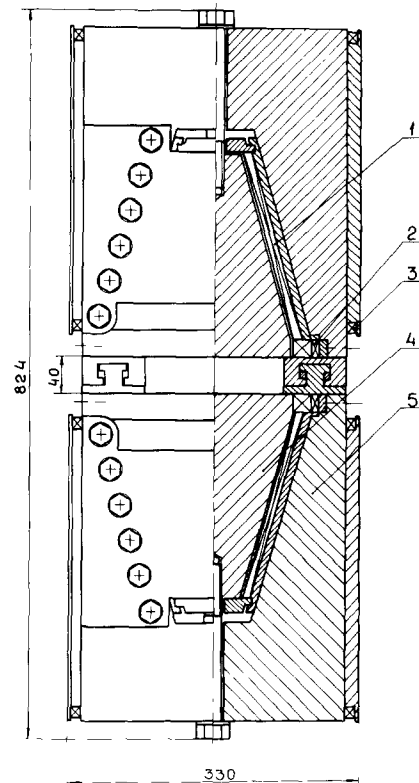


Fig. 3. Layout of a superconducting magnet (without the yoke closing the reverse magnetic flux): (1) major winding, (2) additional winding, (3) compensating winding, (4, 5) iron.

Table 2
Magnet parameters

Interpole gap (cold) [mm]	40
Working aperture [mm ²]	40 × 24
Magnet length [cm]	26
Value of the field [kG]	60
Current in windings 1, 2 and 3 [kA]	2.0, 0.5 and 0.5
Energy content of the magnet [kJ]	200

upper flange by three adjustable suspensions. To avoid the attraction of a magnet to a warm yoke, the helium volume is connected to the warm wall of the cryostat by four horizontal tie-rods. Helium fills any of the cryostats or leaves it by gravity and the helium reservoir is in the centre of the storage ring. The total thermal power flux to the cryogenic system of the storage ring is 11.4 W and corresponds to 400 l helium consumption for 24 hours.

Vacuum in the storage ring is created via condensation by the walls of the helium volumes in superconducting magnets (total area 1.2×10^5 cm²) and also via a complex pumping by means of magnetic discharge pumps and titanium evaporators (total pump rate 10^4 l/h). In this case, the mean pressure of the residual gas in the vacuum chamber of the storage ring is about 10^{-9} Torr at a beam current of about 0.3 A.

2. Injection and rf system

The injection into the storage ring is performed from a linear accelerator at 60 MeV energy. The field in the bending magnets is here $B_{inj} = 6$ kG. At the injection energy, the damping time of betatron and synchrotron oscillations is 1.25 and 0.625 s, respectively. For the injection processes, the repetition frequency is 0.5–1 Hz.

The injection is one-turn and vertical; besides, the prekick is used, and the excited oscillations of the stored beam are completely compensated for in an inflector.

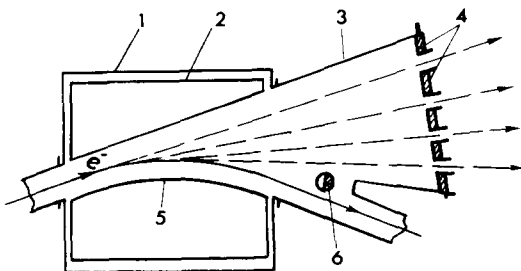


Fig. 4. Scheme of SR extraction from the bending magnet: (1) cryostat body, (2) nitrogen screen, (3) SR extraction chamber, (4) radiation receiver, (5) vacuum chamber in a bending magnet, (6) pinlike radiation receiver.

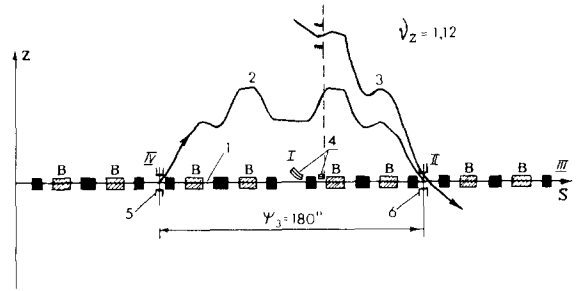


Fig. 5. Injection scheme (1) orbit of the stored beam, (2) trajectory of the stored beam between the pre-inflector and the inflector during the injection, (3) trajectory of the injected beam, (4) input magnets, (5) pre-inflector plates, (6) inflector plates

For injection, two septum magnets are in use. One of them bends the injected beam by 40° , whereas the other bends it by 4° with a thin knife.

Fig. 5 shows the scanning of the storage ring magnetic system along the electron path; the elements of the injection system are indicated. Fig. 6 presents the injection in the normalized phase space of the vertical betatron motion. Here 1, 2, 3 and 4 denote the sequential positions of the stored beam on the phase plane after

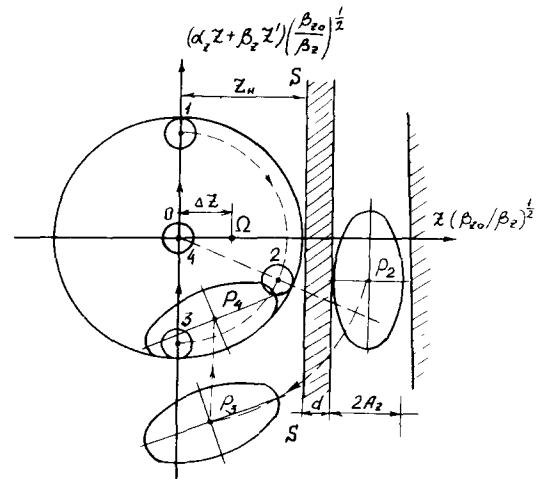


Fig. 6. Phase diagram of the injection

Table 3
Resonator parameters

Working frequency [MHz]	30.0
Characteristic resistance [Ω]	25
Quality factor	6600
Branch resistance [k Ω]	165
Accelerating voltage [kV]	80–100
Maximum power consumed from an rf generator [kW]	40

the kick of the pre-inflector, on the azimuth of injection, at the entrance of the inflector and after the kick of the inflector respectively. P_2 , P_3 and P_4 stand for the centre of the ellipse of the injected beam on the injection azimuth, at the entrance of the inflector and after the kick of the inflector, respectively.

The rf system of the storage ring operates at the first harmonic of the revolution frequency. The rf cavity is of the coaxial type, it is quarter-wave, vacuum, and is strongly shortened by the capacitance. Its parameters are given in table 3.

3. Beam parameters and spectral properties of SR

The lifetime of the electron beam is determined by the Toushek effect, which is the stronger the higher the particle density in the bunch. Fig. 7 illustrates the dependence of the lifetime on the beam current for various amplitudes of the accelerating voltage at 60 and 600 MeV energies. The energy dependence of the beam lifetime is depicted in fig. 8 for the beam current $I = 300$ mA.

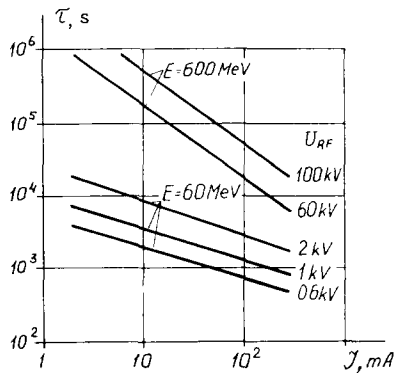


Fig. 7. Calculated lifetime as a function of the beam current.

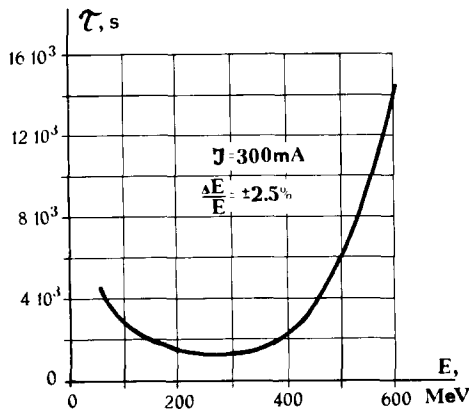


Fig. 8. Calculated lifetime as a function of the energy.

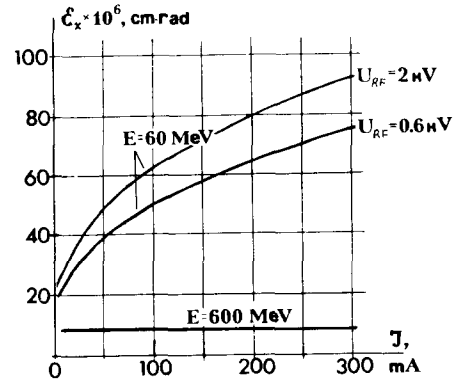


Fig. 9. The horizontal emittance vs the beam current

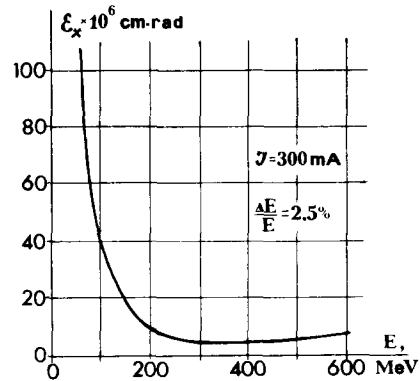


Fig. 10. The horizontal emittance vs the energy.

Figs. 9 and 10 show the horizontal emittance vs the beam current for 60 and 600 MeV energies as well as vs the energy for $I = 300$ mA, which results from a joint action of the Toushek effect and the quantum fluctuations of radiation. At the injection energy, the beam sizes are determined by both the quantum fluctuations of radiation and the multiple Toushek effect. At high energies these are mainly determined by quantum fluctuations of the SR and do not practically depend on the beam current.

The radiation extracted from bending magnets has the critical wavelength $\lambda_c = 8.6 \text{ \AA}$ and the divergence angle in the vertical direction is $\Delta\psi = 1/\gamma = 8.33 \times 10^{-4}$ rad.

The full radiated power is 10.3 kW at 300 mA current. For $E = 600$ MeV and $I = 300$ mA, the luminosity is 1.6 W/cm^2 at a distance of 10 m from the irradiation point.

References

- [1] V.V. Anashin et al., Project for the Storage Ring Siberia-SM, Preprint INP 88-96 (Novosibirsk, 1988).
- [2] L.M. Barkov et al., Application of the Wiggler from Superconducting Magnets to SR Generation at VEPP-3, Preprint INP 78-13 (Novosibirsk, 1978).